

*Electronic Supplementary Information for*

**Structure-adaptive dual-function polyT sequences enable  
homogeneous label-free colorimetric sensing platform**

Shao-Yu Sun<sup>a</sup>, Yi Song<sup>a</sup>, An-Qi Xiao<sup>b</sup>, Xin-Yan Zhang<sup>a</sup>, Xu-Xia Yan<sup>a</sup>, Hui-Dong  
Qiu<sup>a</sup>, Qian-Yu Zhou<sup>a\*</sup>

<sup>a</sup>School of Chemistry and Chemical Engineering, Chongqing University of Science and  
Technology, Chongqing 401331, China.

<sup>b</sup>Chongqing Water & Environment Holdings Group, Ltd., Chongqing, China.

\* Corresponding Author

E-mail addresses: [zhouqy@cqust.edu.cn](mailto:zhouqy@cqust.edu.cn) (Qian-Yu Zhou)

## **Table of contents**

- Fig. S1 The chemical structures of guanine and thymine**
- Fig. S2 The steady-state kinetic analysis of T<sub>10</sub>**
- Fig. S3 The steady-state kinetic analysis of T<sub>16</sub>**
- Fig. S4 The steady-state kinetic analysis of T<sub>36</sub>**
- Fig. S5 Effect of different tert-butanol concentrations on DNA catalysis**
- Fig. S6 Effect of acetate buffer concentration on DNA catalysis**
- Fig. S7 Effect of different buffers on DNA catalysis**
- Fig. S8 CD spectra of T<sub>36</sub> probe with and without melamine**
- Fig. S9 Fluorescence melting curves of T<sub>36</sub> with and without melamine**
- Fig. S10 Determination of binding constants by fluorescence titration method**
- Fig. S11 Effect of acetate buffer concentration on detection of melamine**
- Fig. S12 Effect of acetic acid buffer pH on detection of melamine**
- Fig. S13 Effect of temperature on detection of melamine**
- Fig. S14 Effect of reaction time on detection of melamine**
- Fig. S15 Effect of TMB concentration on detection of melamine**
- Fig. S16 Effect of H<sub>2</sub>O<sub>2</sub> concentration on detection of melamine**
- Fig. S17 Effect of T<sub>36</sub> concentration on detection of melamine**
- Fig. S18 Effect of different Hg<sup>2+</sup> concentrations on DNA catalysis**
- Fig. S19 Effect of nucleases on DNA catalysis**
- Fig. S20 Effect of temperature on DNA catalysis**
- Fig. S21 The change in catalytic activity of T<sub>36</sub> over a 10-day period**
- Table S1 The oligonucleotides used in this work**
- Table S2 Kinetic parameters of poly-T sequences towards TMB**

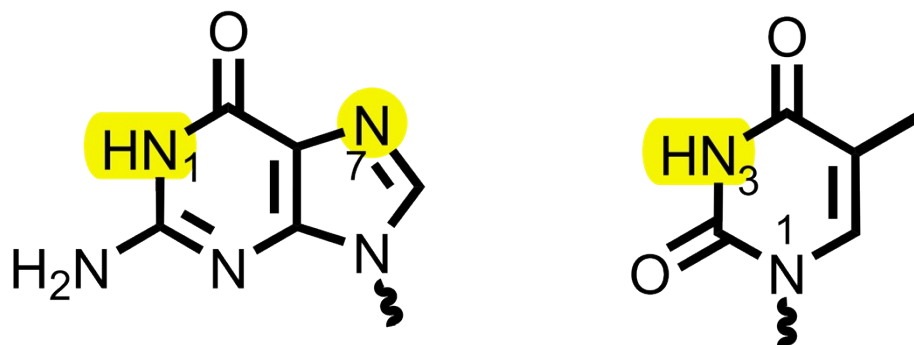


**Fig. S1** The chemical structures of guanine and thymine.

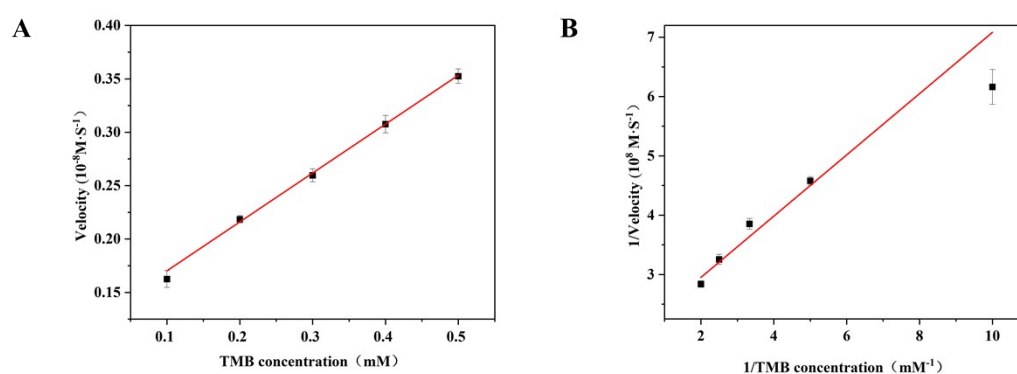


**Fig. S2** (A) The Michaelis-Menten curve of T<sub>10</sub> towards TMB. (B) The corresponding Lineweaver-Burk plots.

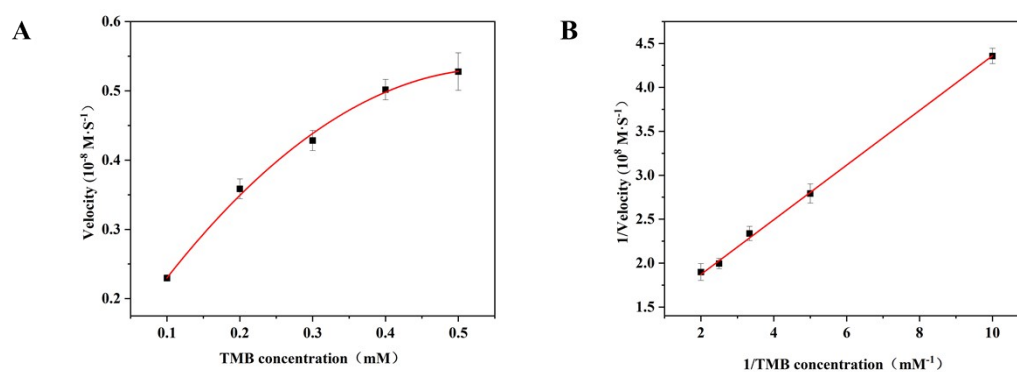


**Fig. S3** (A) The Michaelis-Menten curve of T<sub>16</sub> towards TMB. (B) The corresponding Lineweaver-Burk plots.

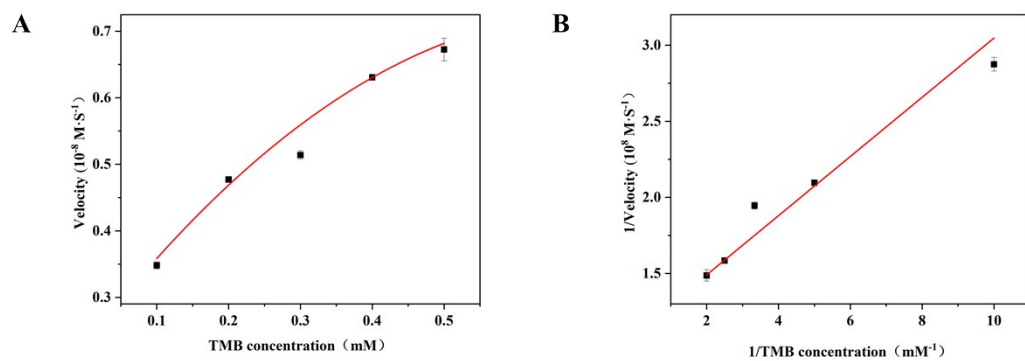


**Fig. S4** (A) The Michaelis-Menten curve of  $T_{36}$  towards TMB. (B) The corresponding Lineweaver-Burk plots.

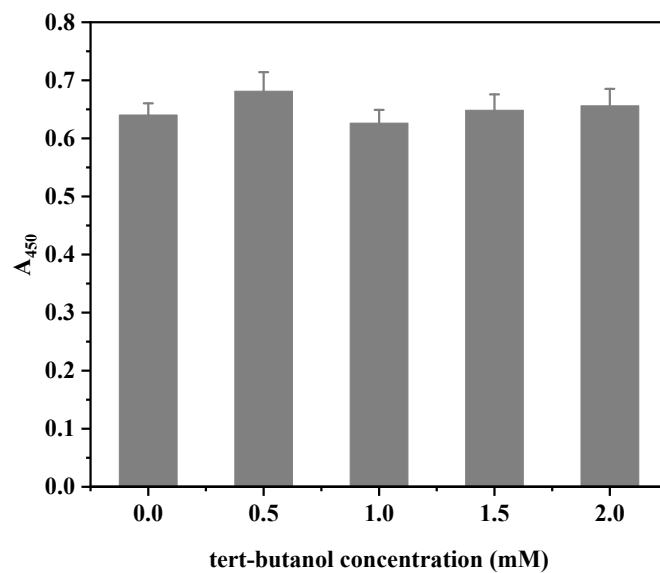


**Fig. S5** Effect of different tert-butanol concentrations on DNA catalysis.

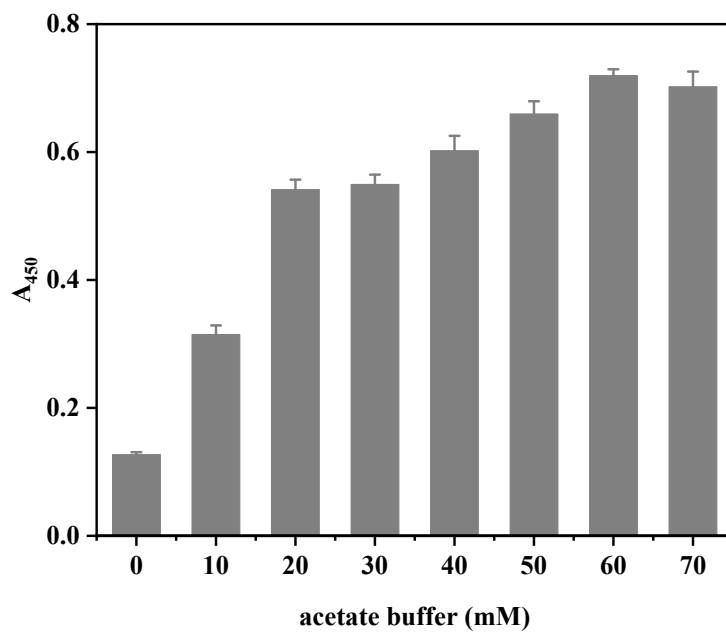


**Fig. S6** Effect of acetate buffer concentration on DNA catalysis.

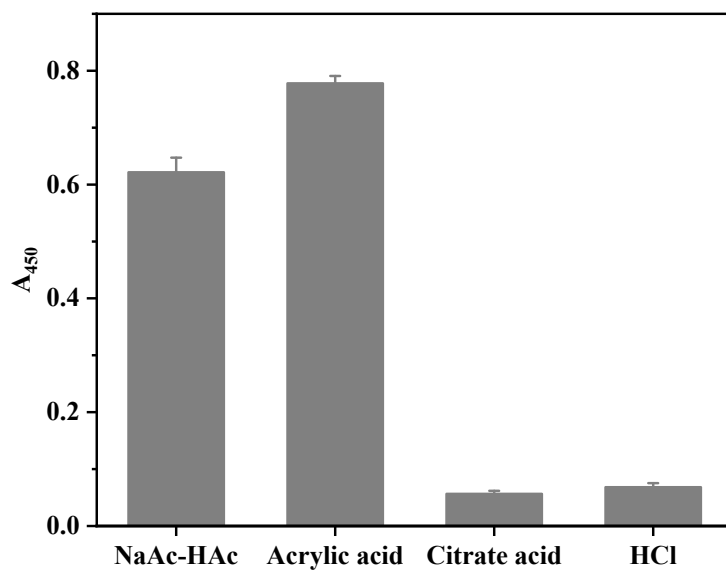


**Fig. S7** Effect of different buffers on DNA catalysis.

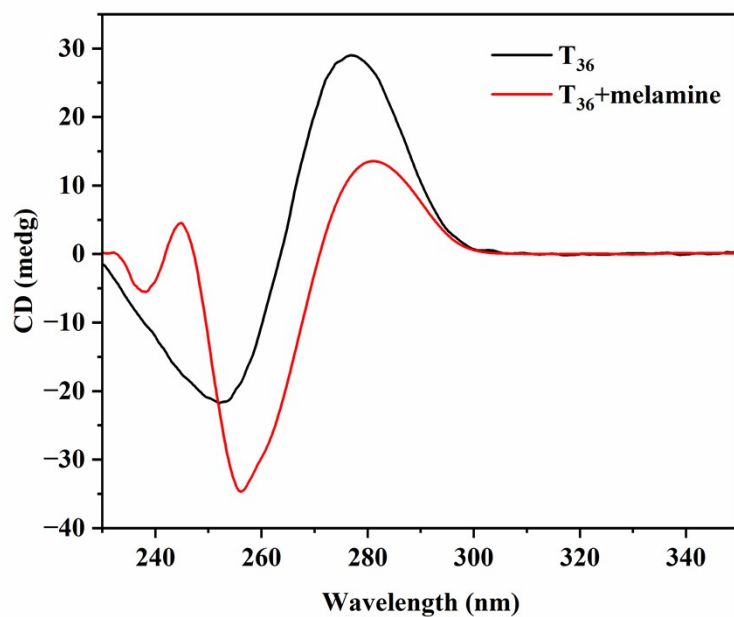


**Fig. S8** CD spectra of  $T_{36}$  probe with and without melamine.

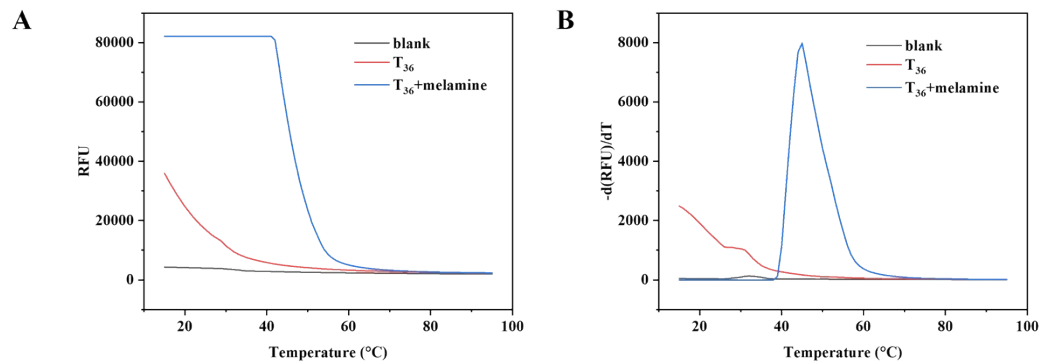


**Fig. S9** (A) Fluorescence melting curves of  $T_{36}$  with and without melamine. (B) The corresponding derivative plots  $T_m$  determination.

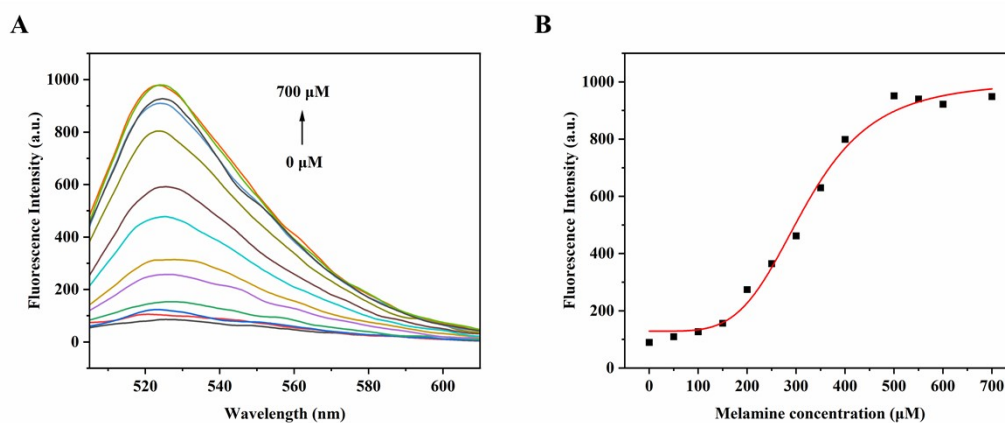


**Fig. S10** (A) Fluorescence titration spectra of the SYBR Green I/poly-T probe with different concentrations of melamine. (B) Plot of fluorescence intensity as a function of melamine concentration.

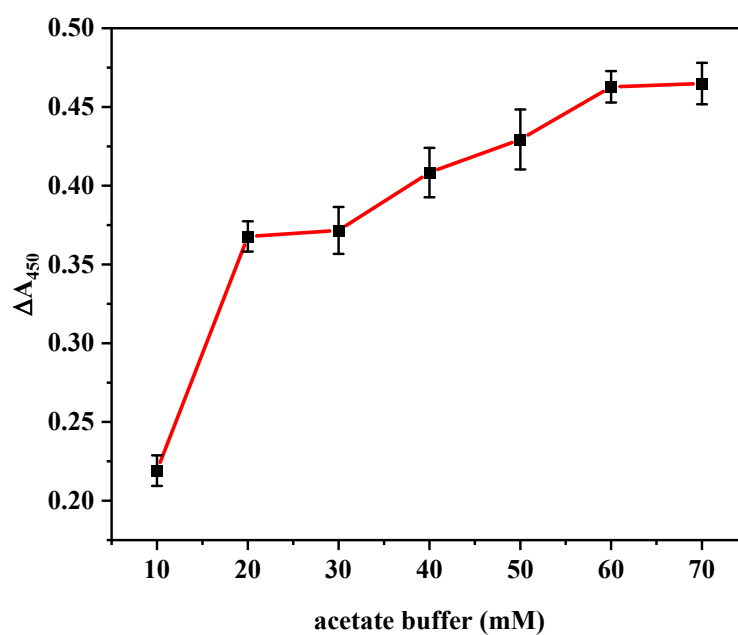


**Fig. S11** Effect of acetate buffer concentration on detection of melamine ( $\Delta A_{450} = A_0 - A_1$ ,  $A_0$  and  $A_1$  correspond to the absorbance values at 450 nm in the absence and presence of melamine, respectively).

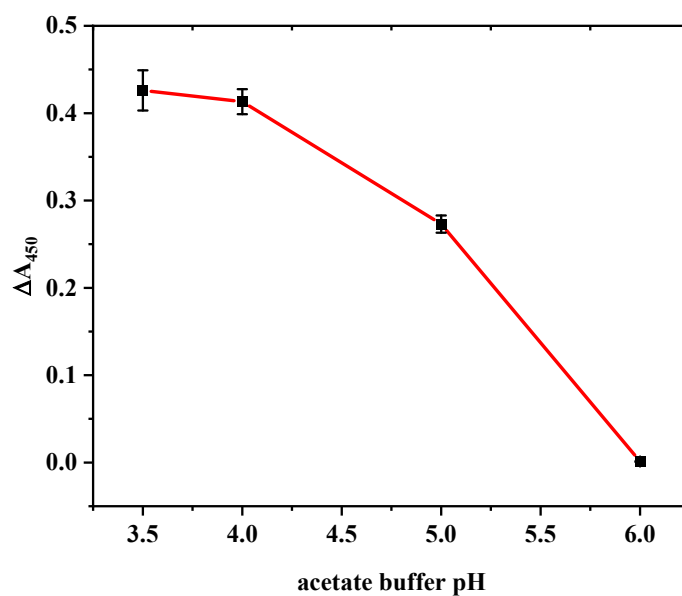


**Fig. S12** Effect of acetic acid buffer pH on detection of melamine ( $\Delta A_{450}=A_0-A_1$ ,  $A_0$  and  $A_1$  correspond to the absorbance values at 450 nm in the absence and presence of melamine, respectively).

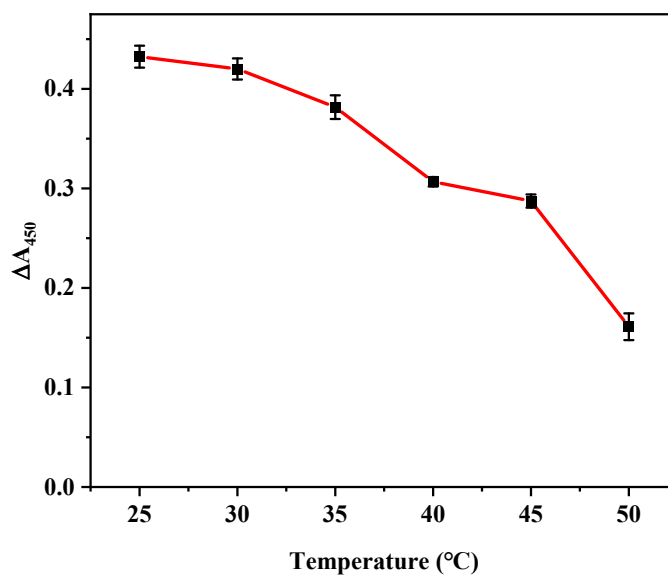


**Fig. S13** Effect of temperature on detection of melamine ( $\Delta A_{450}=A_0-A_1$ ,  $A_0$  and  $A_1$  correspond to the absorbance values at 450 nm in the absence and presence of melamine, respectively).

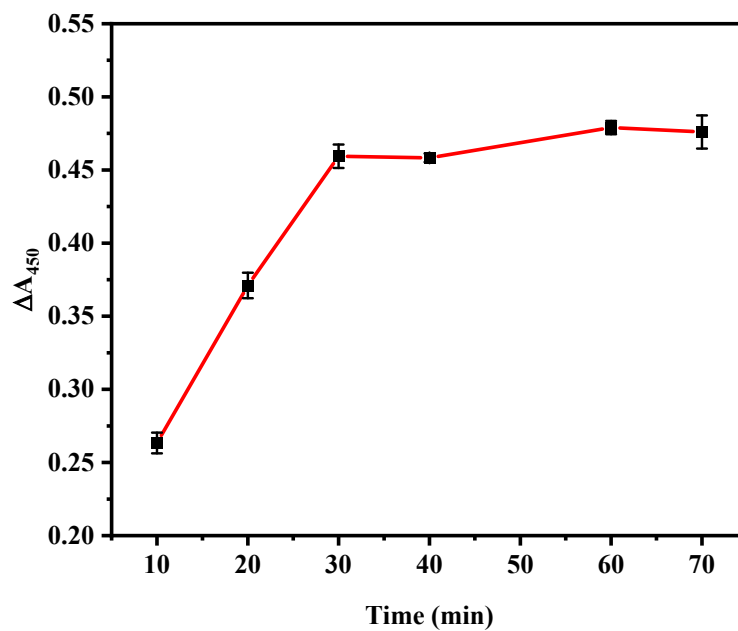


**Fig. S14** Effect of reaction time on detection of melamine ( $\Delta A_{450}=A_0-A_1$ ,  $A_0$  and  $A_1$  correspond to the absorbance values at 450 nm in the absence and presence of melamine, respectively).

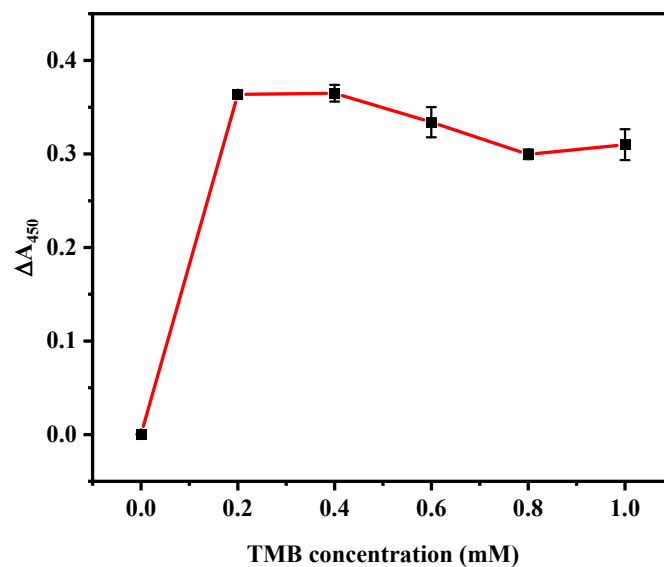


**Fig. S15** Effect of TMB concentration on detection of melamine ( $\Delta A_{450}=A_0-A_1$ ,  $A_0$  and  $A_1$  correspond to the absorbance values at 450 nm in the absence and presence of melamine, respectively).

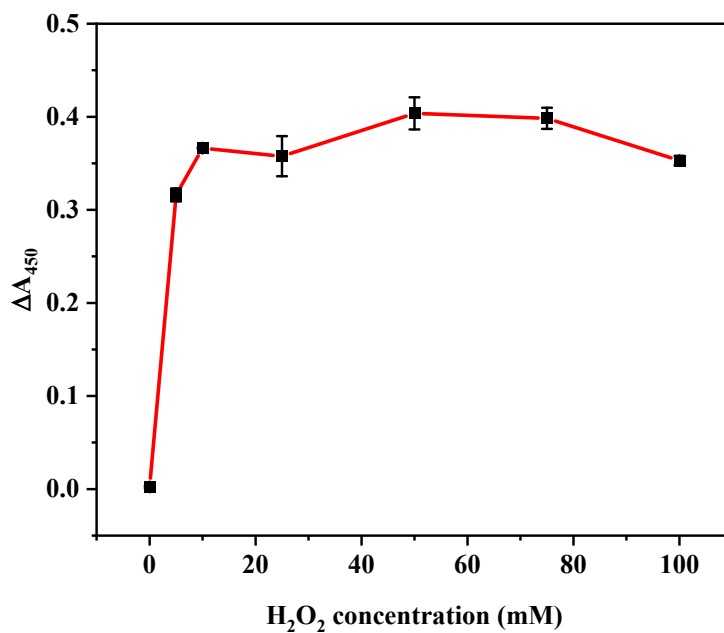


**Fig. S16** Effect of H<sub>2</sub>O<sub>2</sub> concentration on detection of melamine ( $\Delta A_{450}=A_0-A_1$ ,  $A_0$  and  $A_1$  correspond to the absorbance values at 450 nm in the absence and presence of melamine, respectively).

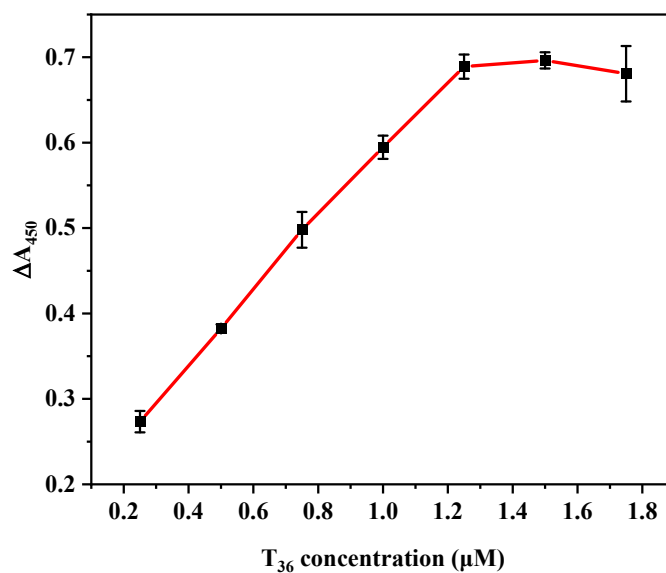


**Fig. S17** Effect of T<sub>36</sub> concentration on detection of melamine ( $\Delta A_{450}=A_0-A_1$ ,  $A_0$  and  $A_1$  correspond to the absorbance values at 450 nm in the absence and presence of melamine, respectively).

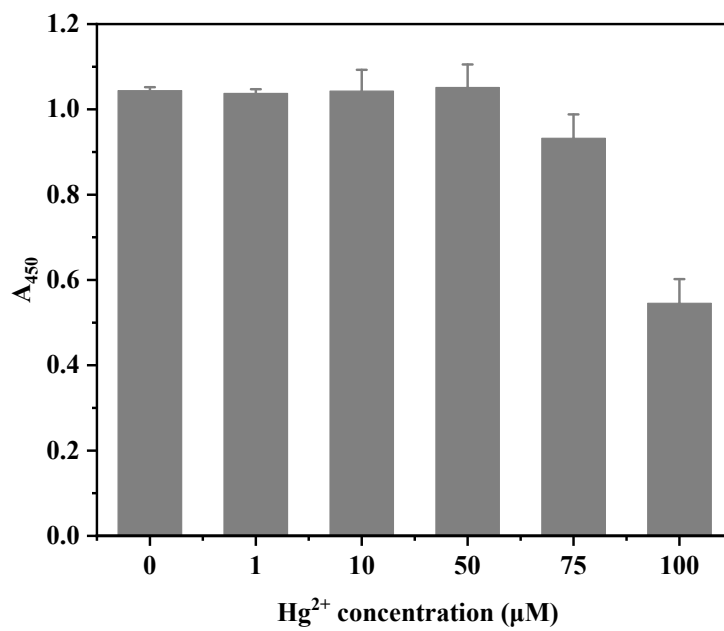


**Fig. S18** Effect of different  $\text{Hg}^{2+}$  concentrations on DNA catalysis.

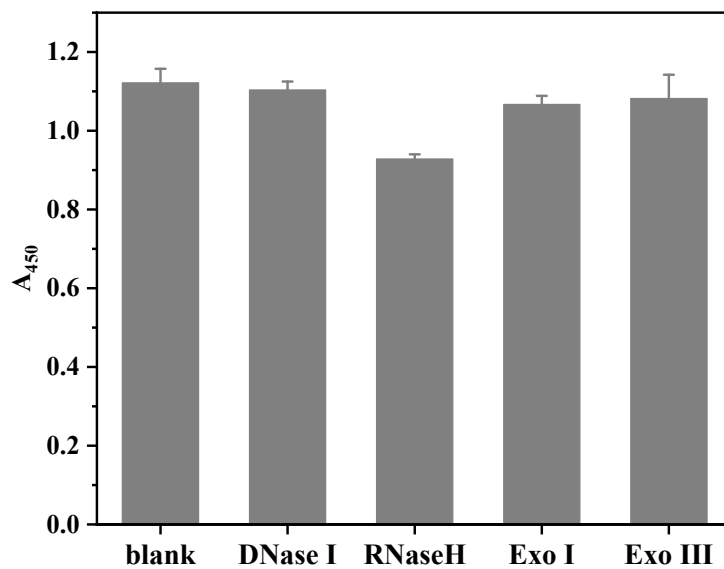


**Fig. S19** Effect of nucleases on DNA catalysis.

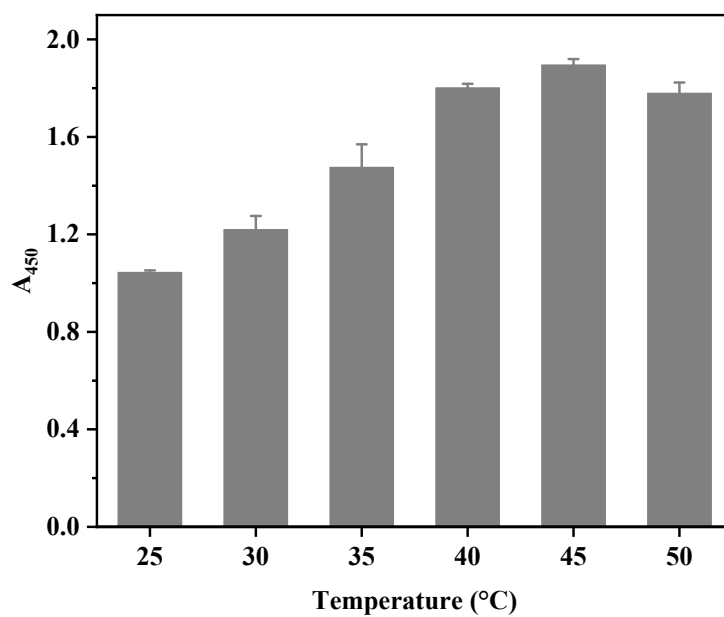


**Fig. S20** Effect of temperature on DNA catalysis.

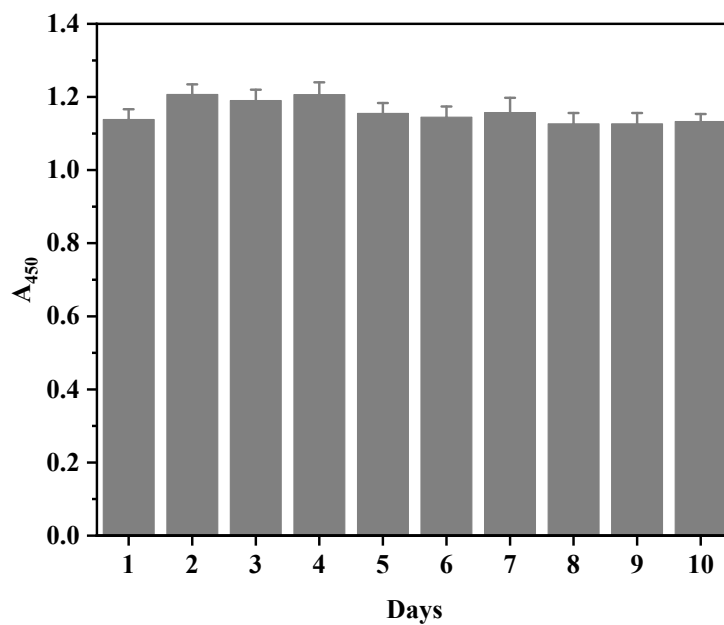


**Fig. S21** The change in catalytic activity of  $T_{36}$  over a 10-day period.

**Table S1 The oligonucleotides used in this work**

Oligonucleotides	Oligonucleotide Sequences
T <sub>10</sub>	5'-TTTTTTTTTT-3'
T <sub>16</sub>	5'-TTTTTTTTTTTTTTTT-3'
T <sub>24</sub>	5'-TTTTTTTTTTTTTTTTTTTTTT-3'
T <sub>36</sub>	5'-TTTTTTTTTTTTTTTTTTTTTTTTTTTTTTTTTT-3'
T <sub>32</sub> C <sub>4</sub>	5'-TTTTTTTTTTTTTTTTTCCCCTTTTTTTTTTTTTTT-3'
T <sub>34</sub> C <sub>2</sub>	5'-TTTTTTTTTTTTTTTTTTCCTTTTTTTTTTTTTTT-3'
T <sub>31</sub> G <sub>2</sub> C <sub>2</sub> A	5'-TTTTTTTTTTTTTTTTTTTTTTTTTTTTTTGGCCA-3'
T <sub>28</sub> C <sub>6</sub> G <sub>2</sub>	5'-TTTTTTTTTTTTTTTTTTTTTTTTTTTCCCCCGG-3'
C <sub>11</sub> G <sub>6</sub> A <sub>3</sub>	5'-CCCCCCCCCGGGGGAAA-3'

**Table S2 Kinetic parameters of poly-T sequences towards TMB**

catalyst	$K_m$ (mM)	$V_{max}$ ( $10^{-9}$ M·S <sup>-1</sup> )
T <sub>10</sub>	0.270	5.22
T <sub>16</sub>	0.249	8.00
T <sub>36</sub>	0.176	9.08